Multicomponent gas analysis using broadband quantum cascade laser spectroscopy

A. Reyes-Reyes,[1,*] Z. Hou,[1] E. van Mastrigt,[2] R. C. Horsten,[1] J. C. de Jongste,[2] M. W. Pijnenburg,[2] H. P. Urbach,[1] and N. Bhattacharya[1]

[1]*Optics Research Group, Faculty of Applied Sciences, Delft University of Technology, Lorentzweg 1, 2628 CJ Delft, Netherlands*

[2]*Department of Pediatric Pulmonology, Erasmus MC-Sophia Children's Hospital, Dr. Molewaterplein 60, 3015 GJ Rotterdam, Netherlands*

[*]*a.reyesreyes@tudelft.nl*

Abstract: We present a broadband quantum cascade laser-based spectroscopic system covering the region between 850 and 1250 cm^{-1}. Its robust multipass cavity ensures a constant interaction length over the entire spectral region. The device enables the detection and identification of numerous molecules present in a complex gas mixture without any pre-treatment in two minutes. We demonstrate that we can detect sub-ppmv concentration of acetone in presence of 2% of water at the same wavenumber region.

OCIS codes: (120.6200) Spectrometers and spectroscopic instrumentation; (140.5965) Semiconductor lasers, quantum cascade; (280.1545) Chemical analysis; (300.1030) Absorption; (300.6340) Spectroscopy, infrared; (300.6360) Spectroscopy, laser; (300.6390) Spectroscopy, molecular.

References and links

1. I. Horvath and J. de Jongste, eds., *Exhaled biomarkers. Eur. Respir. Mon. 2010:49* (European Respiratory Society, 2010).
2. F. K. Tittel and R. Lewicki, "Tunable mid-infrared laser absorption spectroscopy," in *Semiconductor Lasers*, A. Baranov and E. Tournie, eds. (Woodhead, 2013), pp. 579–630.
3. A. Hugi, R. Maulini, and J. Faist, "External cavity quantum cascade laser," Semiconductor Sci. Technol. **25**, 083001 (2010).
4. G. N. Rao and A. Karpf, "External cavity tunable quantum cascade lasers and their applications to trace gas monitoring," Appl. Opt. **50**, A100–A115 (2011).
5. J. H. van Helden, R. Peverall, and G. A. D. Ritchie, "Cavity enhanced techniques using continuous wave lasers," in *Cavity Ring-Down Spectroscopy: Techniques and Applications*, G. Berden and R. Engeln, eds. (John Wiley, 2009), pp. 28–34.
6. D. D. Arslanov, M. Spunei, J. Mandon, S. M. Cristescu, S. T. Persijn, and F. J. M. Harren, "Continuous-wave optical parametric oscillator based infrared spectroscopy for sensitive molecular gas sensing," Laser Photon. Rev. **7**, 188–206 (2013).
7. A. Kosterev, G. Wysocki, Y. Bakhirkin, S. So, R. Lewicki, M. Fraser, F. Tittel, and R. Curl, "Application of quantum cascade lasers to trace gas analysis," Appl. Phys. B **90**, 165–176 (2008).
8. M. C. Phillips, M. S. Taubman, B. E. Bernacki, B. D. Cannon, R. D. Stahl, J. T. Schiffern, and T. L. Myers, "Real-time trace gas sensing of fluorocarbons using a swept-wavelength external cavity quantum cascade laser," Analyst **139**, 2047–2056 (2014).
9. A. A. Kosterev and F. Tittel, "Chemical sensors based on quantum cascade lasers," IEEE J. Quantum Electron. **38**, 582–591 (2002).
10. L. S. Rothman, I. E. Gordon, A. Barbe, D. Chris Benner, P. F. Bernath, M. Birk, V. Boudon, L. R. Brown, A. Campargue, J. P. Champion, K. Chance, L. H. Coudert, V. Dana, V. M. Devi, S. Fally, J. M. Flaud, R. R. Gamache, A. Goldman, D. Jacquemart, I. Kleiner, N. Lacome, W. J. Lafferty, J. Y. Mandin, S. T. Massie, S. N.

#210044 - $15.00 USD Received 11 Apr 2014; revised 12 May 2014; accepted 18 Jun 2014; published 22 Jul 2014

Mikhailenko, C. E. Miller, N. Moazzen-Ahmadi, O. V. Naumenko, A. V. Nikitin, J. Orphal, V. I. Perevalov, A. Perrin, A. Predoi-Cross, C. P. Rinsland, M. Rotger, M. Šimečková, M. A. H. Smith, K. Sung, S. A. Tashkun, J. Tennyson, R. A. Toth, A. C. Vandaele, and J. Vander Auwera, "The HITRAN 2008 molecular spectroscopic database," J. Quant. Spectrosc. Radiat. Transfer **110**, 533–572 (2009).
11. S. W. Sharpe, T. J. Johnson, R. L. Sams, P. M. Chu, G. C. Rhoderick, and P. A. Johnson, "Gas-phase databases for quantitative infrared spectroscopy," Appl. Spectrosc. **58**, 1452–1461 (2004).
12. Block Engineering, "LaserScope user manual" (2012).
13. J. B. McManus, P. L. Kebabian, and M. S. Zahniser, "Astigmatic mirror multipass absorption cells for long-path-length spectroscopy," Appl. Opt. **34**, 3336–3348 (1995).
14. G. O. Nelson, *Gas Mixtures; Preparation and Control* (Lewis, 1992).
15. A. A. Kosterev, R. F. Curl, F. K. Tittel, R. Köhler, C. Gmachl, F. Capasso, D. L. Sivco, and A. Y. Cho, "Transportable automated ammonia sensor based on a pulsed thermoelectrically cooled quantum-cascade distributed feedback laser," Appl. Opt. **41**, 573–578 (2002).
16. A. A. Kosterev, F. K. Tittel, R. Köhler, C. Gmachl, F. Capasso, D. L. Sivco, A. Y. Cho, S. Wehe, and M. G. Allen, "Thermoelectrically cooled quantum-cascade-laser-based sensor for the continuous monitoring of ambient atmospheric carbon monoxide," Appl. Opt. **41**, 1169–1173 (2002).
17. S. E. Braslavsky, "Glossary of terms used in photochemistry, 3rd edition (IUPAC Recommendations 2006)," Pure Appl. Chem. **79**, 293–465 (2007).
18. E. J. Moyer, D. S. Sayres, G. S. Engel, J. M. St. Clair, F. N. Keutsch, N. T. Allen, J. H. Kroll, and J. G. Anderson, "Design considerations in high-sensitivity off-axis integrated cavity output spectroscopy," Appl. Phys. B **92**, 467–474 (2008).
19. M. S. Taubman, T. L. Myers, B. D. Cannon, R. M. Williams, and J. F. Schultz, "Ultra-trace chemical sensing with long-wave infrared cavity-enhanced spectroscopic sensors," Pacific Northwest National Laboratory, Richland, Washington (Technical Report, 2003).
20. A. L. Buck, "New equations for computing vapor pressure and enhancement factor," J. Appl. Meteorol. **20**, 1527–1532 (1981).
21. D. Nelson, J. Shorter, J. McManus, and M. Zahniser, "Sub-part-per-billion detection of nitric oxide in air using a thermoelectrically cooled mid-infrared quantum cascade laser spectrometer," Appl. Phys. B **75**, 343–350 (2002).
22. http://www.massflow-online.com/faqs/what-do-lnmin-lsmin-slm-and-sccm-stand-for/.
23. C. Deng, J. Zhang, X. Yu, W. Zhang, and X. Zhang, "Determination of acetone in human breath by gas chromatography-mass spectrometry and solid-phase microextraction with on-fiber derivatization," J. Chromatogr. B **810**, 269–275 (2004).

1. Introduction

Detection of trace levels of gases is an integral part of life in modern societies. The ability to detect trace gases in real time or offline plays a major role in industrial processes, environmental monitoring, medical diagnostics [1], security, air quality monitoring besides other applications. For this reason and to be able to identify specific molecules, many optical techniques have been developed based on spectroscopy like long path absorption spectroscopy, cavity enhanced spectroscopy, cavity ring down spectroscopy, photoacoustic spectroscopy to name a few. The main advantage offered by spectroscopy is that specific molecules can be identified using their distinctive fingerprints. This can be beneficial when several molecular species are present simultaneously in the gas being analysed. The devices which have been developed for this purpose can be based on high sensitivity, looking for parts per million by volume (ppmv), parts per billion by volume (ppbv) and even parts per trillion by volume (pptv) concentrations of a specific gas, or on a broad band technique which looks for many species simultaneously. These optical techniques are non invasive and very little pre-processing is needed in most cases.

Most devices for spectroscopic gas detection are based on absorption by the molecular species as described by the Beer-Lambert law. Therefore to optimize the sensitivity of the device, the illumination source wavelength and the interaction length have to be carefully chosen. Many systems are based in the near to mid-infrared region of the electromagnetic spectrum. This is mainly because the fundamental rovibrational absorption modes of the molecules produce strong spectroscopic fingerprints in this region [2]. In the near infrared region of the spectrum a host of sources of varying complexity, size and price exist because of the needs of the telecommunication industry for which this is the favored wavelength. However the spectro-

#210044 - $15.00 USD Received 11 Apr 2014; revised 12 May 2014; accepted 18 Jun 2014; published 22 Jul 2014

scopic fingerprints of molecules found in this region are 1000 times weaker than the fundamental absorption modes located in the mid-infrared. Sources in the mid-infrared are scattered over the entire wavelength range (3-24 μm) and are of varying types such as gas lasers, color center lasers, difference frequency generation, optical parametric oscillators, lead salt diodes and the recently developed quantum cascade lasers (QCLs), among others. The quantum cascade lasers which have been developing very fast in recent years are rapidly filling the holes in the wavelength axis, making them an attractive light source for gas analysis [3, 4]. Most QCLs have a well-defined central wavenumber and a narrow linewidth that allow an accurate molecular identification.

The next important element is the optimization of the interaction length between the light and the gas volume. In this case considering that sometimes the gas volume is limited, the choice is generally made to concentrate the light in the volume confining the gas using specifically designed optical cavities. The cavities are designed with two different methodologies namely, they can be resonant cavities or multipass cavities. The resonant cavities offer the possibility to obtain interaction distances in the order of kilometers inside volumes lower than a liter. However the resonators have strong constraints that make their implementation difficult. They require mirrors with reflectivities higher than 99.9% to achieve the needed finesse [5, 6]. Although such mirrors are available with the right reflectivity, their bandwidth is still limited to a few nanometers in the mid-infrared. Another restriction resonators have is the need of a feedback system to correct the position of the mirrors because they are susceptible to small mechanical and thermal changes. Furthermore it is necessary to couple the transversal mode of the laser to the cavity mode. Multipass cavities, on the other hand, only allow interaction distances of tens of meters but their requirements are less demanding. The mirrors' reflectivity is lower, but their working bandwidth is much broader. Multipass cavities are more robust to mechanical and thermal changes eliminating the need of a feedback system.

The combination of QCLs' relatively high power and adequate optical cavities has been successfully used to implement highly sensitive spectroscopic techniques such as cavity ring down, photoacoustics spectroscopy, wavelength modulation spectroscopy and integrated cavity output spectroscopy [6, 7]. Some of these techniques have demonstrated sensitivities in the orders of ppmv, ppbv and pptv levels. However, these techniques only focus on the detection of one or two selected molecules mainly because they only use a small range of the QCLs' tunability bandwidth. By using the full QCLs' tunability it is possible to detect and differentiate the components present in a more complex molecular mixture [8].

In this work we report a broad band spectroscopic trace gas analysis device that covers the atmospheric window between 850 and 1250 cm^{-1} (8 - 11.76 μm) [9]. Our approach targets the simultaneous detection and identification of several molecules present in the gas volume, exploiting the fact that the molecular spectra in this region have a broad profile. We compare the detected spectral profile of the gas mixture with well established molecular databases, like HITRAN [10] and the Pacific Northwest National Laboratory (PNNL) database [11] and identify the specific molecules. Furthermore, the multipass cavity employed in our system allows us to detect concentrations in the ppmv and sub-ppmv levels.

2. Experimental setup

A schematic overview of the experimental setup is shown in Fig. 1. Its main components are: a laser source, a multipass cavity to enhanced the absorption and two detectors to monitor the laser intensity and to measure the absorption signal after the multipass cavity. A visible laser distance-meter (Leica DISTO D2) co-aligned with the laser is used as guiding beam and to measure the interaction distance inside the multipass cavity.

The laser source is part of a LaserScope unit from Block Engineering. It consists of two co-

#210044 - $15.00 USD Received 11 Apr 2014; revised 12 May 2014; accepted 18 Jun 2014; published 22 Jul 2014

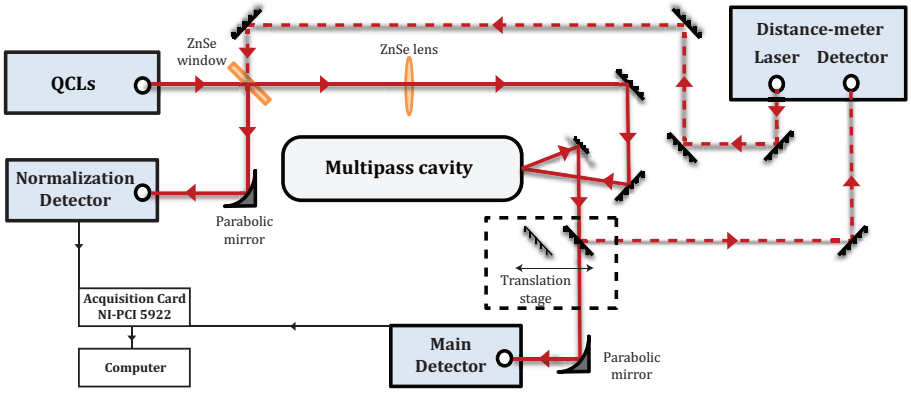

Fig. 1. Schematic overview of the experimental setup. The translation stage allows to switch between the cavity length determination and the measurement configurations.

aligned tunable QCLs. One QCL covers the region between 850 cm^{-1} and 1010 cm^{-1} and the second QCL emits in the region between 1010 cm^{-1} and 1250 cm^{-1}. The QCLs use diffraction gratings in a Littrow configuration with back extraction to tune the wavenumber [12]. The angular position of the grating is controlled using a piezoelectric component. Therefore, the emmited wavenumber is calibrated with the voltage applied to the piezo. The QCLs wavenumber accuracy is 0.1 cm^{-1}. The QCLs' average power varies between 0.5 and 12 mW depending on the emitted wavenumber. Both QCLs are pulsed, with a pulse repetition rate of 200 kHz and the pulses have a temporal width of 208 ns. These parameters are optimum for the emission of the QCLs in terms of intensity and stability. We use pulsed QCLs because they have stable operation at room temperature.

The multipass cavity is based on the modified Herriot configuration described by McManus et. al. [13]. It consists of two 2.5 in. (1 in. = 2.54 cm) astigmatic mirrors (Aerodyne Research, Inc.) with a reflectivity $r > 0.983$ over the full spectral range of the QCLs. The distance between the mirrors measured along the optical axis is 32.4 cm. The mirrors are placed on custom made mounts inside a stainless steel vacuum cell. The cell has an input ZnSe window (Thorlabs WG71050-F) with a transmission $t > 0.95$ in the working spectral range. The number of reflections n inside the cavity determines the interaction path-length achievable but it also defines the amount of light coming out of the cavity through the intensity reduction coefficient k,

$$k = t^2 r^n. \tag{1}$$

Even though this type of cavities allow interaction lengths of up to 100 meters [13] we prefer a configuration with an interaction length of 54.36 meters, which is long enough to detect molecules in concentrations levels of few ppmv and at the same time provides a strong output signal. The power coming out of the multipass cell is 5.5% of the laser power sent into the cell. The total volume of the cell is 0.6 liters. The multiple reflections and the compact configuration allows the laser to travel through most of the volume of the cell, which allows a homogeneous interaction with the entire gas sample.

We use a pressure controller (Bronkhorst, P-702CV-1K1A-RAD-22-V) and a diaphragm vacuum pump (Vacuubrand MD 1) to control the pressure inside the cavity. The pressure measurements are particularly important for molecules whose spectra contain sharp absorption lines. Such lines can suffer broadening because of different effects, for example collisional or Doppler broadening. To control the injection of samples inside the cell we use a set of mass flow con-

#210044 - $15.00 USD Received 11 Apr 2014; revised 12 May 2014; accepted 18 Jun 2014; published 22 Jul 2014

trollers (Bronkhorst, F-201CV-1K0-RAD-22-V), which allows us to prepare samples with the desired concentrations using single and double dilution techniques [14].

For the detection we use two thermo-electric cooled (TEC) Mercury Cadmium Telluride (MCT) detectors and a fast acquisition card (NI-PCI 5922). As depicted in Fig. 1 the main detector collects the signal emerging from the multipass cavity. The 100 MHz cut-off frequency of this detector (VIGO System, PVI-4TE-10.6-0.3x0.3-TO8-BaF2) and the 10 mega samples per second (MS/s) sampling rate of the acquisition card allows to detect the peak power of each pulse, increasing the signal to noise ratio (SNR) of the measurement [9]. A second detector (LaserScope unit, Block Engineering) is necessary to monitor the laser intensity directly outside the QCLs and normalize the intensity of each pulse. This normalization minimizes the pulse to pulse intensity variation of the QCLs and increases the sensitivity of the system [15, 16].

3. Multipass characterization

3.1. Robustness

In most multipass cavities the allowed input angle of the incoming laser beam has a small tolerance. Our configuration increases the tolerance using a 500 mm ZnSe lens in front of the multipass cavity. As explained before, the broadband tunability of our QCLs is obtained using a Littrow configuration with back extraction, which reduces the wavenumber-dependent angular displacement of the laser beam to less than 3 mrad. To demonstrate the robustness of our device we produced pulses with a temporal width of 112 ns and measured the normalization signal and the signal from the cavity using one detector. For this experiment the configuration of Fig. 1 was modified to place both signals on the main detector. We only used one detector to have the same detection response and avoid any electronic delay. The signal was analysed using a RIGOL DS1102E oscilloscope. We repeated this measurement for three different central wavenumbers as shown in Fig. 2. In all cases the delay between signals is 185 ns when the cavity is empty, confirming that all pulses travel the same distance inside the cavity. In particular the angular displacement between the pulses of Figs. 2(b) and 2(c) is maximum, which confirms the tolerance of the multipass cell.

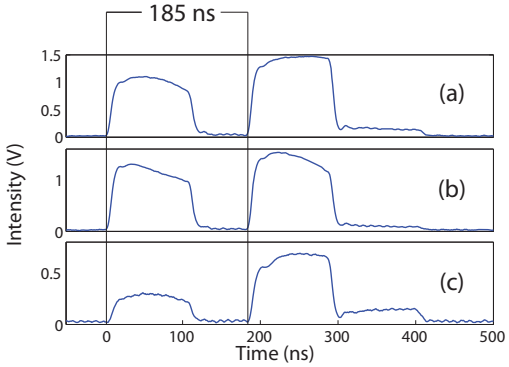

Fig. 2. Delay time between the normalization and the main signals for three different wavenumbers. (a) 950 cm^{-1}, (b) 1000 cm^{-1} and (c) 1150 cm^{-1}.

3.2. Internal path-length determination

To measure the path-length inside the multipass cavity we used two methods. First we used the laser distance meter, averaged 50 measurements and subtracted the path the laser travels outside the cavity, getting a path-length of 54.36 meters. Then we used the 185 ns pulse delay between

#210044 - $15.00 USD Received 11 Apr 2014; revised 12 May 2014; accepted 18 Jun 2014; published 22 Jul 2014

the normalization and the main signal shown in Fig. 2. Subtracting the distance traveled by the laser outside the cavity we got a measured distance of 54.33 meters. These two independent measurements are consistent. The 3 cm difference between them represents a delay of 100 ps which we cannot resolve using our oscilloscope.

4. Measurements

For the absorption measurements we first build a reference spectra $I_0(\nu)$, where ν is the wavenumber. For that we record the transmission of a laser scan through the multipass cavity with vacuum or filled with a neutral gas which has no absorption lines in the spectral region of our device. Then we average the result of ten laser scans. Immediately after, we introduce the gas sample inside the cavity to minimize the effects on our measurements induced by atmospheric variations outside the cavity. Then we scan the laser ten times and average the signal to construct a measurement spectrum $I_m(\nu)$. Using the Beer-Lambert law [17] we obtain the absorbance $A(\nu)$ of the sample,

$$A(\nu) = -\log_{10}\left(\frac{I_m(\nu)}{I_0(\nu)}\right). \tag{2}$$

The absorbance can also be written in terms of the molecular concentration C in ppmv, the interaction path-length between the light and the molecules ($l = 54.36$ meters in the case of the present device) and the molecular absorption coefficient $\varepsilon(\nu)$ in ppmv^{-1}m^{-1}, which is an intrinsic property of the material,

$$A(\nu) = \varepsilon(\nu) C l. \tag{3}$$

Using this last relation we can determine the molecular concentration from the strength of the absorbance.

4.1. Noise determination and sensitivity analysis

The noise level of our system is determined comparing two reference spectra. As they are taken with an empty cavity the variations are only induced by the laser and detector fluctuations. The ratio between two reference spectra is a good comparison and as we are interested in the absorbance we can use directly Eq. (2). From this result the noise level is established by taking the absorbance root mean square (rms) value. For our system it has a value of 0.02.

To determine the performance of our system we used the formalism developed by Moyer et. al. [18]. The minimum detectable absorption per scan (MDA_{ps}) is given by

$$MDA_{ps} = \left(\frac{\Delta P}{P}\right)_n \sqrt{n}\sqrt{T_{scan}}. \tag{4}$$

Where $\Delta P/P$ correspond to the rms level calculated above, the number of scans integrated, n, is equal to 10 and the time a single scan takes, T_{scan}, is equal to 5.3 s. The MDA_{ps} for our system has a value of 0.14 Hz$^{-1/2}$. To compare with systems that scan over a narrower or broader spectral region is important to defined the minimum detectable absorption per point (MDA_{pp}). As we have a well-defined number of datapoints, $\#pts = 8000$, we use the data acquisition rate, $r_{data} = \#pts/T_{scan}$ as our relevant bandwidth. In this case the $MDA_{pp} = MDA_{ps}/(\#pts)^{-1/2}$ and has a value of 1.6 $\times 10^{-3}$Hz$^{-1/2}$. The comparison with systems with different interaction path-lengths is better done using the noise equivalent absorption sensitivity (NEAS) [18, 19]. Since the interaction distance inside the cavity, l, was determined to be 54.36 meters the $NEAS = MDA_{pp}/l$ and gives a value of 2.99 $\times 10^{-7}$cm^{-1}Hz$^{-1/2}$

#210044 - $15.00 USD Received 11 Apr 2014; revised 12 May 2014; accepted 18 Jun 2014; published 22 Jul 2014

4.2. *Specific gas measurements*

In this section we present a series of measurements to show the performance of our setup. In these measurements the reference spectrum was taken with vacuum of 0.10 mbar inside the cavity. In all cases we use an atmosphere of N_2 as buffer for the sample gas mixture because N_2 does not have absorption lines in the spectral range of the present device. The first two measurements correspond to controlled mixtures of acetone and ethanol. The mixtures were obtained using a double dilution process [14]. This way we could cross-check the concentration of the samples. We choose these molecules because they have strong and smooth absorption profiles in our spectral region. Then we prepared a single dilution mixture of CO_2 to study the wavenumber resolution and the sensitivity of our system, because CO_2 has a lower absorption in our region. Finally we present the measurement of two complex mixtures to show the applications of our method.

4.2.1. Acetone, ethanol and CO_2 spectra

In Fig. 3(a) the measured spectrum of acetone with a concentration of 22 ppmv at 900 mbar in an atmosphere of N_2 is shown in red. The black line corresponds to the acetone spectrum in the same wavelength region from the PNNL database. In this case there are broad features that can be easily identified, they are centered at 900 cm^{-1} and 1218 cm^{-1}.

In Fig. 3(b) we present the measured spectrum of ethanol with a concentration of 60 ppmv at 900 mbar in an atmosphere of N_2, in red. The black line corresponds to the ethanol spectrum in the same wavelength region from the PNNL database. In this spectrum the experimental setup captures the finer spectral details, such as the peaks at 1028, 1038, 1058 and 1066 cm^{-1}. In this case there is a mismatch in the region between 980 cm^{-1} and 1020 cm^{-1} corresponding to the transition between the two QCLs. But this is not a limitation to detect the desired molecules since the main spectroscopic features are clearly identifiable.

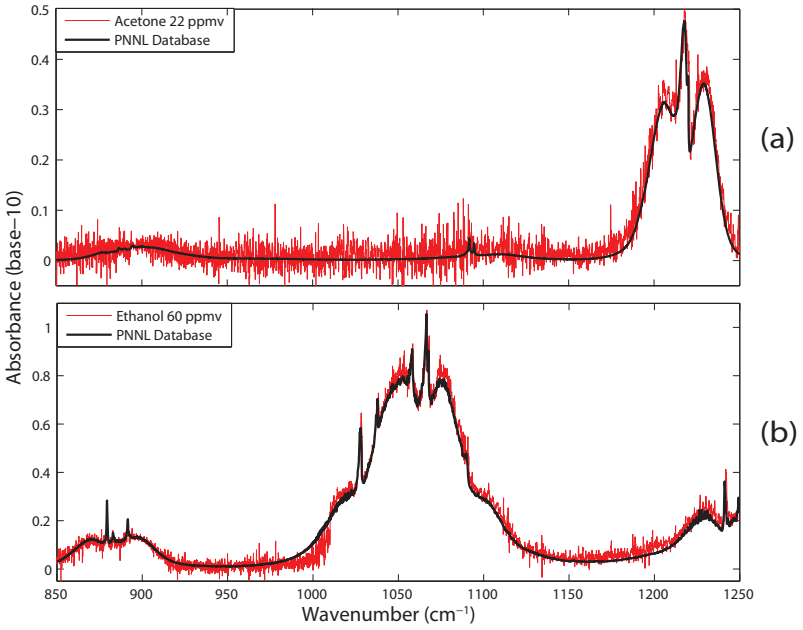

Fig. 3. Absorption spectrum of 22 ppmv of acetone and 60 ppmv of ethanol. Both at 900 mbar in an atmosphere of N_2.

#210044 - $15.00 USD Received 11 Apr 2014; revised 12 May 2014; accepted 18 Jun 2014; published 22 Jul 2014

Furthermore, from a measurement of a 15% concentration of CO_2 at 500 mbar in an atmosphere of N_2 we could resolve the rovibrational spectrum as shown in Fig. 4(a). The observed CO_2 absorption lines are four orders of magnitude weaker than the strongest absorption lines of CO_2. However, when we compare the spectrum with the theoretical information contained in the HITRAN database we notice that the strength of the absorbance does not match with the information contained in the database, Fig. 4(b). This effect is due to the wavenumber accuracy of our device, which is too large to correctly retrieve the profile of each absorption line. Therefore, it is not possible to directly measure the strength of each absorption line and the sample concentration. To determine the sample concentration we first fit a Voigt profile to each individual absorption line, then we compare the maxima of the peaks with the HITRAN database using Eq. (3) to obtain a concentration value for each peak. We thus have several concentration values calculated for different lines of the same molecule. The mean value of these concentrations give us the sample concentration. From this analysis we obtained a 15% concentration of CO_2 with a standard deviation of 5%.

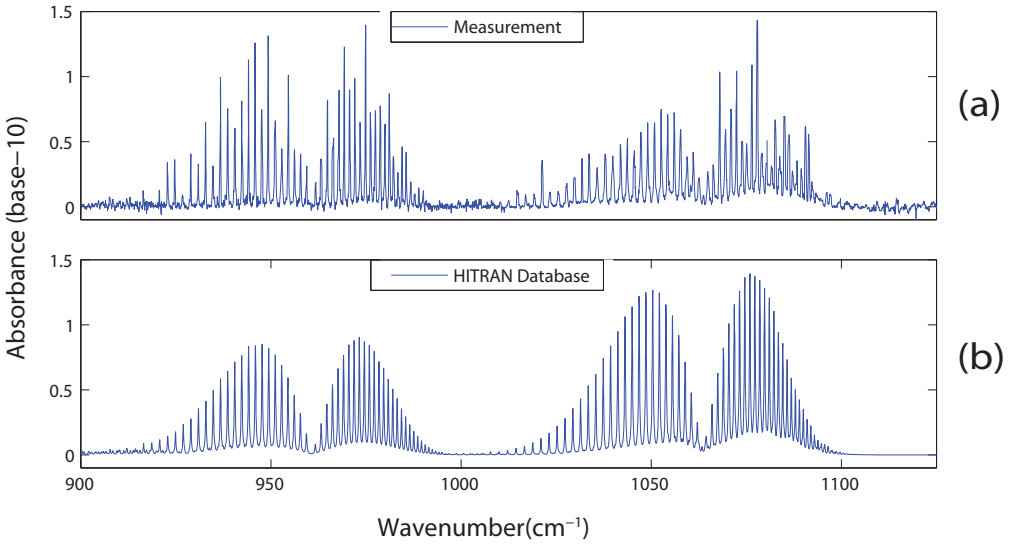

Fig. 4. Spectrum of 15% of CO2 in an atmosphere of N_2 at 500 mbar. (a) Experimental measurement. (b) HITRAN database.

These measurements show some of the system's advantages and limitations. The broadband coverage of the system allows the molecular identification of molecules with a smooth spectral profile because all the available absorption features are used, this permits to determine the sample concentration in a couple of minutes. For molecules with sharp spectral features the identification is possible but the concentration determination strongly depends on the absorption strength.

4.2.2. Lab air spectrum

An easy test for our setup is the measurement of the environment from our lab. For this purpose we filled the multipass cavity with lab air and obtained the absorbance depicted in Fig. 5. In this spectrum we can clearly observe five absorption lines of water at 1136 cm^{-1}, 1175 cm^{-1}, 1187 cm^{-1}, 1212 cm^{-1} and 1225 cm^{-1}. As in the case of CO_2 there is a mismatch between the strength from some measured spectral lines and the HITRAN database. Again the main reasons for this mismatch is the fact that we are observing absorption lines three

#210044 - $15.00 USD Received 11 Apr 2014; revised 12 May 2014; accepted 18 Jun 2014; published 22 Jul 2014

orders of magnitude weaker than the strongest water absorption lines and the wavenumber accuracy mentioned previously. However, using the method described above we determined a concentration of 1% with a standard deviation of 0.7%, which reflects how the magnitude of the absorption strength of the molecule improves the concentration determination.

To obtained an independent measurement of the water concentration in the lab air we used a Vaisala transmitter (PTU300). It allowed us to measure the atmospheric pressure $P = 1001.0$ mbar, the relative humidity $RH = 31.0\%$ and the temperature $T = 23.0°\mathrm{C}$ in the lab. With this information we calculated the saturated pressure of water vapour p_w^* using the relation [20],

$$p_w^* = \left[1.0007 + (3.46 \times 10^{-6} P)\right] \times (6.1121) \exp\left[\frac{17.502T}{240.97+T}\right] \tag{5}$$

and then we calculated the concentration in percentage,

$$C_w = \frac{p_w^* RH}{P}. \tag{6}$$

From this independent measurement we obtained a concentration of 0.9%. This value is consistent with the spectroscopic measurement obtained using our device. The main source of error is the uncertainty in the strength of the absorption signal due to the wavenumber spacing.

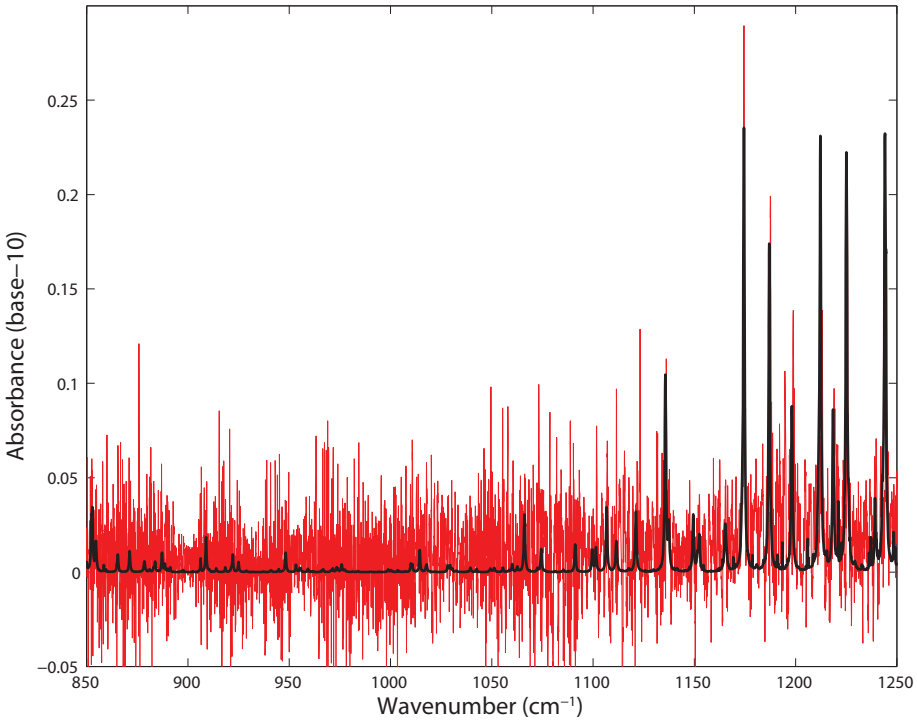

Fig. 5. Lab air sample at 1001.0 mbar, at a temperature of 23.0 °C and a relative humidity of 31.0%. In black is depicted the spectrum of water from HITRAN database with a concentration of 1 %.

#210044 - $15.00 USD Received 11 Apr 2014; revised 12 May 2014; accepted 18 Jun 2014; published 22 Jul 2014

4.2.3. Breath sample

Finally we measured a breath sample from a healthy volunteer from our research group. The pressure inside the multipass cavity was 900 mbar and there was a continuous flow of the sample at 500 milliliter normal per minute (ml_n/min) [22]. As seen in Fig. 6, we could resolve the absorption lines of CO_2 with a concentration of 3% and water at 2%. An interesting feature is the shift upwards of the base line in the region between 1170 and 1250 cm^{-1} as shown by the red curve in the inset of Fig. 6. In this region there is absorption from water and acetone. The black line in the inset of Fig. 6 shows the water absorption and the 500 ppbv of acetone, giving a better match to the red curve corresponding to the measured spectrum. This concentration of acetone is in the normal range for a healthy person [23].

This measurement demonstrates the capability of the system to detect the presence of several molecules in a single sample. Using the overall profile allows to make an accurate and fast initial molecular identification of molecules with high concentrations. By examining closely the baseline of the spectrum we can identify and observe molecules with broad and smooth absorption profile. Their presence shifts the spectrum baseline and allows us to detect sub-ppmv concentrations.

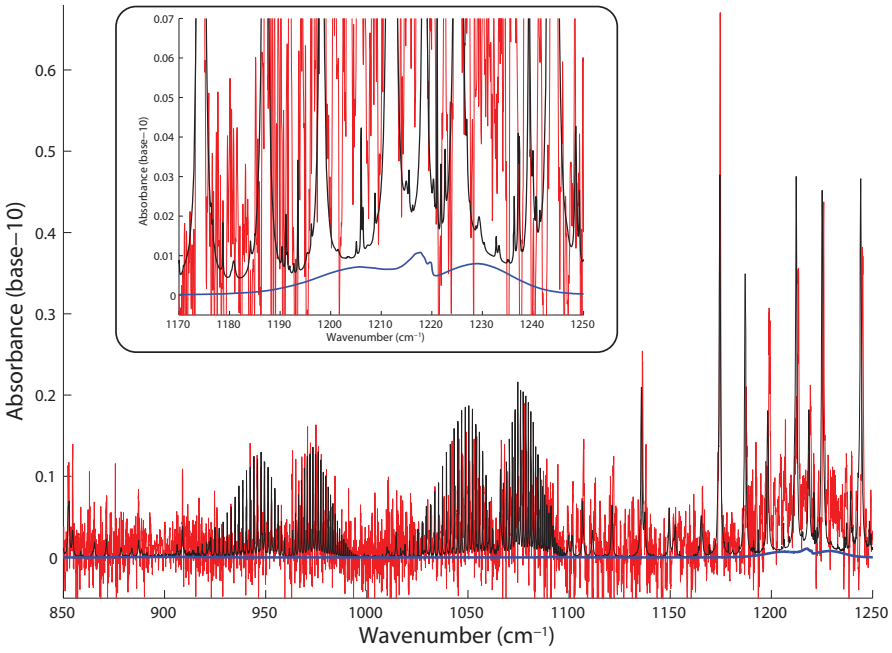

Fig. 6. Breath sample at 900 mbar and flowing at 500 ml_n/min. In black is depicted the theoretical spectrum with 3% of CO_2 and 2% of water from HITRAN database and 500 ppbv of acetone from the PNNL database. In blue is the spectrum of acetone with a concentration of 500 ppbv taken from PNNL database.

5. Conclusions

In this work we present a broadband spectroscopic gas analysis device which covers the molecular fingerprint region between 850 and 1250 cm^{-1}. It complements the direct absorption spectroscopic systems available in the 1250 - 3000 cm^{-1} region. At the same time broadens the

#210044 - $15.00 USD Received 11 Apr 2014; revised 12 May 2014; accepted 18 Jun 2014; published 22 Jul 2014

spectral bandwidth covered by one single setup. This device enables the study of complex gas mixtures because the robustness of the multipass cavity guarantees a stable interaction length over the full spectral scan. For applications requiring sensitivities in the ppmv and hundreds of ppbv levels this system is ideal to quickly estimate the composition of a gas sample without any pre-treatment. The sensitivity characterization gave us a *NEAS* of $2.99 \times 10^{-7} \mathrm{cm}^{-1}\mathrm{Hz}^{-1/2}$. Furthermore, the sensitivity can be increased by a factor of 10 by incrementing the delay introduced by the multipass cavity and measuring the absorption and the normalizing signal in one single detector [21].

The most important feature of the system is the fast identification of molecules with a broad and smooth spectral profile as shown with the acetone signature in the breath sample measurement. This shows that our system is reliable for applications such as the detection of molecular markers in complex gas mixtures like breath. Specially for cases where the concentration levels are in the order of hundreds of ppbv or higher.

Acknowledgments

We gratefully acknowledge Rob Pols and Alonso Millan-Mejia for the design and construction of the vacuum cell used for the multipass cavity. We also thank Thim Zuidwijk and Vincent Docter for their valuable help with the experiment. This project was funded by the Dutch Foundation for Fundamental Research on Matter (FOM) through the project 09NIG20-1.

#210044 - $15.00 USD Received 11 Apr 2014; revised 12 May 2014; accepted 18 Jun 2014; published 22 Jul 2014